ChemComm

Cite this: DOI: 10.1039/c0xx00000x

www.rsc.org/xxxxxx

COMMUNICATION

Solvent effect in an axially symmetric Fe^{III}_4 single-molecule magnet†

Yuan-Yuan Zhu,[a,b] Ting-Ting Yin,[a] Shang-Da Jiang,*[c,d] Anne-Laure Barra,[d] Wolfgang Wernsdorfer,[e] Petr Neugebauer,[f] Raphael Marx,[f] María Dörfel,[f] Bing-Wu Wang,[b] Zong-Quan Wu,[a] Jorisvan Slageren,*[f] Song Gao*[b]

Received (in XXX, XXX) Xth XXXXXXXXX 20XX, Accepted Xth XXXXXXXXX 20XX
DOI: 10.1039/b000000x

A pair of enantiopure Fe^{III}_4 SMMs with axial symmetry were synthesized and characterized by magnetization and high-frequency electron paramagnetic resonance methods. The result reveals that the axial symmetry of the structure is broken by the interaction of the Fe^{III}_4 and the disordered solvent molecules.

Molecular magnetism is a highly multidisciplinary area between chemistry, physics and materials science, and has been so since the discovery of single-molecule magnets (SMM).[1] Currently, scientists are making great efforts to manipulate individual or monolayer of SMM so as to develop molecular spintronics.[2] The structural instability of well-studied Mn_{12} family turns out to be an obstacle in such development, while the Fe^{III}_4 clusters have become outstanding candidates due to their enhanced structural and redox stabilities.[3,4] Most of the reported Fe^{III}_4 clusters are based on the tripodal ligand synthetic strategy.[5-8] As a variation, we have recently provided a new approach by employing chiral Schiff base ligand L = (*R* or *S*)-2-((2-hydroxy-1-phenylethylimino)methyl)-4-R-phenol (R = H, Cl, Br, I, *t*-Bu) These ligands can be extensively modified in appropriate positions. This adaptability allows tuning the relaxation energy barrier,[9] provides the possibility of anchoring to surfaces and generating long-range-ordered molecular arrays. All the previously reported Fe^{III}_4 molecules are of low symmetry, which introduces transverse terms in the effective spin Hamiltonian mixing the ground doublet and causing efficient quantum tunneling of magnetization (QTM). Herein, we report a further member of the Fe^{III}_4 with high symmetry.

The compounds **1*R*** and **1*S*** $[Fe^{III}_4(L^{R\text{ or }S})_6]$·X DMA (X = 9 for **1*R*** and 7 for **1*S***) were obtained as dark red crystals from the reaction of $FeCl_2$, H_2L ((*R* or *S*)-2-((2-hydroxy-1-phenylethylimino)methyl)-4-nitrophenol) and Et_3N in methanol and recrystallized in hot DMA (*N*,*N*-dimethylacetamide) (see ESI†). The enantiopure *R* and *S* ligands were obtained from the reaction of chiral source, and afterwards the chiral pure ligands were employed to synthesize the complexes. The enantiopure complexes are obtained directly. The X-ray single-crystal structural analysis (Figure 1) reveals that **1*R*** and **1*S*** are enantiomers and crystallize in the trigonal class *R*32 with the absolute structure parameters (Flack parameter) being 0.084 for **1*R*** and 0.003 for **1*S***. The central and peripheral Fe^{III} ions are located on the C_3 and C_2 rotation axis, respectively. There are only two independent magnetic centres within the molecule. The overall symmetry of the molecule is of the point group D_3. Due to the C_2 rotation axis, the helical pitch angle of the Fe^{III}_4 core is 90°. The DMA solvent molecules are highly-disordered in the unit cell, due to their low symmetry. According to the location of the electron densities, we propose that the solvent molecules crystallize along the C_3 axis and peripherally between the molecules. Since it is not possible to refine the solvent molecule structure reasonably, we squeezed the solvent electron density out by PLATON program for clarity.[10] The short contacts between adjacent molecules can be identified between the oxygen of NO_2 group and hydrogen from aromatic rings of neighbouring clusters.

Due to the rigidity of the ligand, the chirality is successfully transferred and amplified from the ligand to the coordination environment of Fe^{3+} ions. The Fe/O skeleton exhibits specific propeller-like chirality, in which **1*R*** is in a (Δ) configuration and **1*S*** is in a (Λ) one. The optical activity and enantiomeric nature of **1*R***/**1*S*** were also confirmed by circular dichroism (CD) spectra in both solution and solid state (Figure S2.3-2.4).

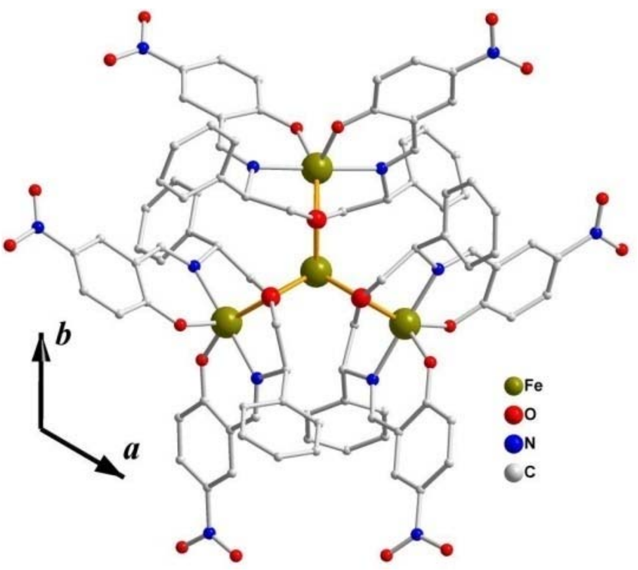

Fig.1 The structure of **1*R*** viewed along ***c*** axis. Hydrogen atoms are omitted for clarity.

Static and dynamic magnetization measurements were performed on both powder crystals of **1*R*** and **1*S***. This pair of enantiomers exhibit identical magnetic responses to static and alternative field, therefore, all the magnetic discussions below are focused only on R enantiomers. The magnetic susceptibility was measured at1000 Oe static field. The temperature dependence of the magnetic susceptibility of**1*R***is plotted in Figure 2, indicating a strong antiferromagnetic interaction with incomplete spin cancellation. The $\chi_M T$ value is 12.02 cm^3 K mol^{-1} at 300 K and decreases on cooling till around 160 K with a minimum of 11.01 cm^3 K mol^{-1}, and then increases to the value of 14.75 cm^3 K mol^{-1} at 20 K. Below this temperature, a sharp decrease is observed. These results indicate the occurrence of an antiferromagnetic coupling between the central high spin Fe^{III} ion (s = 5/2) and the three peripheral high spin Fe^{III} ions (s = 5/2), resulting in a ground state of S = 5. The observed $\chi_M T$ value of **1*R*** at the low temperature maximum (14.75 cm^3 K mol^{-1}) is in good agreement with the value of 15.00 cm^3 K mol^{-1} expected for S = 5 with g = 2.0.

The 3-fold symmetry nature leads to two kinds of magnetic interactions within one molecule, named J_1 and J_2, representing the exchange coupling between the central and peripheral Fe^{III} ions, and within peripheral ones, respectively. The HDVV spin Hamiltonian can be expressed as:

$$\boldsymbol{H} = -2J_1(\boldsymbol{S}_1\cdot\boldsymbol{S}_2 + \boldsymbol{S}_1\cdot\boldsymbol{S}_3 + \boldsymbol{S}_1\cdot\boldsymbol{S}_4) - 2J_2(\boldsymbol{S}_2\cdot\boldsymbol{S}_3 + \boldsymbol{S}_3\cdot\boldsymbol{S}_4 + \boldsymbol{S}_4\cdot\boldsymbol{S}_2) + g\mu_B\boldsymbol{S}\cdot\boldsymbol{B} \quad (1)$$

The magnetic susceptibility data was fitted with the above Hamiltonian by MAGPACK.[11] The best fitting of the data in the temperature range 20–300 K of **1*R*** provides J_1 = −11.7(1) cm^{-1} and J_2 = 0.33(1) cm^{-1},confirmingthe antiferromagnetic interaction between the central and peripheral Fe^{III} ions and weak ferromagnetic coupling interaction between adjacent peripheral Fe^{III} ones.

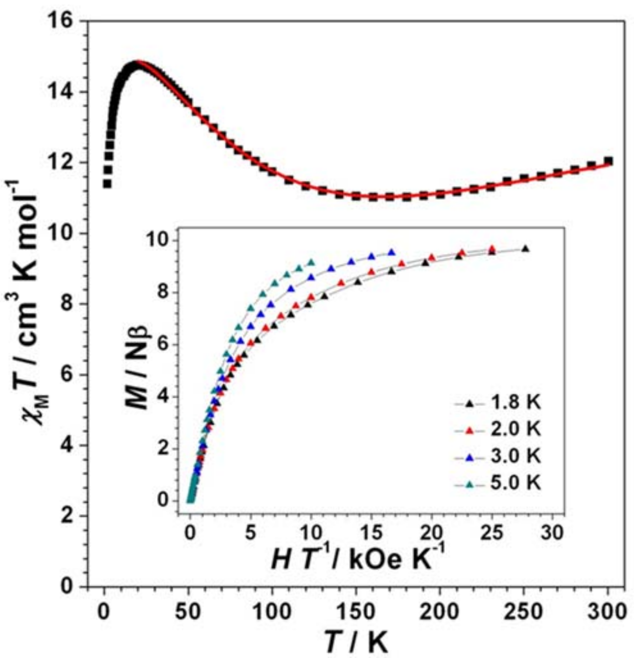

Fig. 2 Temperature dependence of $\chi_M T$ (the red solid line was calculated with the best-fit parameters reported in the text.*H*/*T* plots at different temperatures (1.8, 2.0, 3.0, and 5.0 K) for the polycrystalline sample of **1R**.

Isothermal magnetization data were collected in field up to 5 Tat various temperatures (1.8, 2.0, 3.0, and 5.0 K). The M *v.s.* H/T curves display significant bifurcation(inset of Figure 2), indicating the presence of an appreciable magnetic anisotropy in the ground state. Considering the anisotropy of the spin ground state with the effective spin Hamiltonian $\boldsymbol{H} = D\boldsymbol{S}_z^2 + g_{iso}\mu_B\boldsymbol{S}\cdot\boldsymbol{B}$, the magnetic data was fitted by the program ANISOFIT 2.0.[12]The axial anisotropy parameter $D$is determined to be −0.38(1) cm^{-1}.

HFEPR is one of the most powerful approaches to determine the ZFS parameters in molecular magnetism. HFEPR spectra of **1*R***powder sample were recorded at10 and 15 K and 220.8 and 331.2GHz (Figure 3(a) and S6.1). In both the frequencies at 15 K two groups of lines can be observed corresponding to the magnetic field parallel and perpendicular to the quantized axis in the low- and high-field regions. The line intensities in the parallel region move to lower fields upon cooling, revealing a negative sign of D. The spectra can be well reproduced with the S = 5 effective spin Hamiltonian consistent with the magnetic data, and the transition with the strongest intensity at base temperature can be attributed to |–5> to |–4>. The best simulation of the spectra at both frequencies and temperatures are obtained to be g_{iso} = 2.00,D = –0.369(1) cm^{-1} and E< 0.001 cm^{-1}, consistent with the magnetic study. The simulations of the spectra are performed with the consideration of Gaussian distribution of both D and E, whose FWHM values are 0.01 and 0.03 cm^{-1}, respectively.

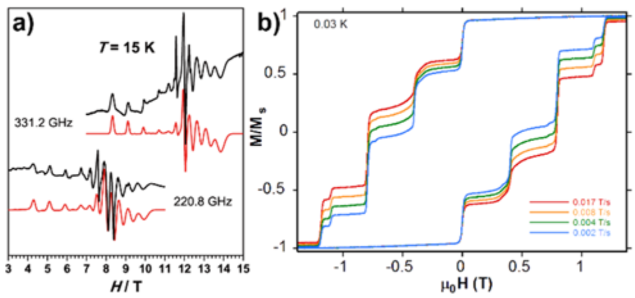

Fig. 3(a)Experimental (black) and simulated (red) HFEPR spectra of **1*R***powder sample at 15 K.The simulation was carried out with the easyspin toolbox for Matlab.[16] (b) The magnetic hysteresis of **1*R*** single crystal at various field sweeping rates at 0.03 K. The magnetic field was applied along the magnetic easy axis of the single crystal.

However, the HFEPR spectrum on a single crystal sample is rather surprising compared with the powder data. The crystal is well aligned with its crystallographic ***c*** axis along the magnetic field. At 15 K, six groups of parallel transitions, corresponding to the transition between |– m> to |– m +1>, are visible in Figure 4a, where m can be integer between 0 and 5, as marked. Interestingly, each transition consists of three peaks, indicating there are at least three sorts of Fe^{III}_4 molecules in the single crystal with different but similar ZFS parameters. Furthermore, the transitions are broadened at lower field, implying a distribution of the parameters. This spectrum is simulated with three D values (–0.356(1), –0.342(1) and –0.331(1) cm^{-1}) of different weights (80%, 15% and 5%, respectively), where each D is considered to have a Gaussian distribution with a full width at half maximum(FWHM) value of 0.007 cm^{-1}. The spectrum with the field applied in the hard plane was also recorded on the same crystal at 15 K (Figure 4b). The line broadening is more obvious at high field region. Taking the D values and weights determined from the parallel orientation, one can reproduce the spectrum with E= 0.004 cm^{-1} and the Gaussian distribution FWHM = 0.01

cm^{-1} for all the three components. The spectra from rotating the magnetic field in the hard plane are plotted in Figure S6.2. The static field is applied at an angle θ from the crystallographic ***a*** axis (face index information in Figure S6.3).The transition lines do not show obvious angular dependence, due to the rather wide E distribution. This is compatible with the fact that the local 3-fold symmetry of the Fe^{III}_4 is removed by its interaction with the solvent molecules.

Since the three Fe^{III}_4 molecules in the unit cell are equivalent by symmetry, we believe that the existence of these three components is due to the interaction of the molecules with differently oriented disordered solvent molecules. This is similar to $Mn_{12}OAc$, where the disordered acetic acid molecules create four types of hydrogen bonds with the $Mn_{12}OAc$ molecule, destroying the 4-fold symmetry.[13]In the present case, a similar analysis is not applicable, since the solvent molecules are highly disordered. This solvent-disorder effect may also give rise to the observed D and E distribution. Furthermore, it is rather interesting to realize that all of these D parameters determined from single crystal are much smaller than the one, either from magnetic or HFEPR studies, of powder sample. This is very probably due to the loss of solvent molecules in the powder sample. Even if this solvent-loss will very probably destroy the 3-fold symmetry of the molecule, no peak splitting is observed in the perpendicular transitions in Figure 3a, therefore the second rank transverse spin Hamiltonian parameter E is less than 0.001 cm^{-1}. Nevertheless, this does not conclude that the 3-fold symmetry holds in the powder sample. Since the line shapes are broadened intensively, a wider distribution of the parameters is expected, as reported aforementioned.

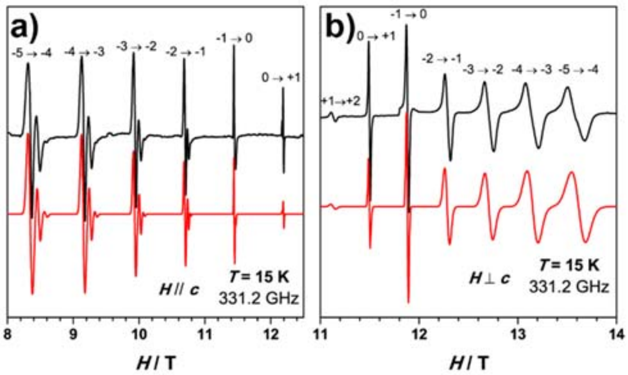

Fig. 4 Experimental (black) and simulated (red) HFEPR spectra of **1*R*** single crystal sample at 15 K. The magnetic field was applied along (a) and perpendicular (b) to the crystallographic ***c*** axis. The labels above the peaks indicate the eigenstates involved in the transitions.

It has been revealed that the rigid skeleton of the Fe^{III}_4 molecule determined by the single crystal X-ray diffraction is of perfect D_3 symmetry, while an individual Fe^{III}_4 molecule interacts with the disordered solvent molecules unsymmetrically, meaning that the Fe^{III}_4 local symmetry is reduced from its skeleton D_3 point group. This can be evidenced from the micro-SQUID measurement on a single crystal.

The magnetic field was scanned along the single crystal ***c*** axis at various sweeping rates at 0.03 K, which is low enough to avoid obvious thermal excitation. It can be seen in Figure 3b that an evident QTM step is recorded around zero field. This is not achievable for $S = 5$ system with pure D_3 symmetry within giant spin model, since the ground doublet states (|±5>) are orthogonal and can't be mixed by any sort of 3-fold symmetry. The aforementioned solvent-disorder effect is able to introduce the second rank transverse anisotropy term, and is responsible for the QTM at zero field. The loops at various sweeping rates show a rather wide level crossing field range, indicating the distribution of molecular environments in this single crystal, which is consistent with HFEPR result.[14] According to the averaged level crossover, one can calculate the D parameter from hysteresis, yielding a value of –0.35 cm^{-1}.

The magnetic bistability behavior can also be verified by the zero-field-cooled (ZFC) and field-cooled (FC) magnetization in a small field (Figure S4.4). The ZFC and FC curves split below 0.8 K, suggesting that, below that temperature, the orientation of the overall axial molecular magnetic moment is frozen along the magnetic easy axis direction on the timescale of the experiment.

Dynamic magnetic susceptibility measurements characterize the magnetic relaxation process of SMMs. For compound **1*R***, both the in-phase (χ') and out-of-phase (χ'') susceptibilities show frequency dependence below 3 K in the absence of a static field (Figure S5.1-5.2). The Arrhenius analysis provides $\tau_0 = 1.6 \times 10^{-7}$ s and U_{eff} = 14.1(4) K (Figure S5.3), comparable to the theoretical value ($U_{eff} = |D|S^2$= 13.3 K) within the experimental error limit, where D is taken from the powder EPR spectrum. This compound shows the most significant magnetic hysteresis and highest energy barrier among the reported analogues.[9]Thelarger $|D|$, leading to larger easy axial anisotropy, is responsible for this enhancement.

In conclusion, a pair of high symmetric Fe^{III}_4 SMMs has been synthesized and characterized, whose spin Hamiltonian parameters are determined by magnetic and HFEPR methods. The results show that this pair of compounds is of strong easy axial anisotropy possessing the highest blocking temperature in this Fe^{III}_4 family reported by us. Even if the molecular skeleton shows a perfect 3-fold symmetry, the highly disordered solvent molecules destroy this pure axial anisotropy. This solvent effect is also confirmed by the single crystal HFEPR and micro-SQUID measurement. It worth noting that, other than the solvent effect, a phase transition below the temperature where we determined the crystal structure could be a source of the symmetry reduction as well. The high symmetry is of interest because it can provide us the possibility to investigate the origin of magnetic anisotropy.[15]We are now pushing to recrystallize the molecule in various solvents and modify the ligand, so as to get rid of the solvent effect.

We acknowledge the support of the Natural Science Foundation of China (21290171, 21321001, 21302035, and 21371043), the National Basic Research Program (2013CB933401), the Alexander von Humboldt Stiftung (S.-D. J. Postdoc research fellow actions).S.-D. J. is grateful for the support of Prof. Martin Dressel and Dr. Lapo Bogani from 1. Physikalisches Institut, Universität Stuttgart. Y.-Y. Z. is thankful for the financial support by the Open Fund of Beijing National Laboratory for Molecular Sciences (BNLMS).

Notes and references

1. R. Sessoli, D. Gatteschi, A. Caneschi and M. A. Novak, *Nature*, 1993, **365**, 141.
2. L. Bogani and W. Wernsdorfer, *Nat. Mater.*, 2008, **7**, 179.
3. L. Margheriti, M. Mannini, L. Sorace, L. Gorini, D. Gatteschi, A. Caneschi, D. Chiappe, R. Moroni, F. B. de Mongeot, A. Comia, F. M. Piras, A. Magnani and R. Sessoli, *Small*, 2009, **5**, 1460.
4. (a) M. Mannini, F. Pineider, Ph. Sainctavit, C. Danieli, E. Otero, C. Sciancalepore, A. M. Talarico, M.-A. Arrio, A. Cornia, D. Gatteschi and R. Sessoli, *Nat. Mater.*, 2009, **8**, 194; (b) M. Mannini, F. Pineider, C. Danieli, F. Totti, L. Sorace, P. Sainctavit, M. A. Arrio, E. Otero, L. Joly, J. C. Cezar, A. Cornia and R. Sessoli, *Nature*, 2010, **468**, 417.
5. (a) A. L. Barra, A. Caneschi, A. Cornia, F. F. de Biani, D. Gatteschi, C. Sangregorio, R. Sessoli and L. Sorace, *J. Am. Chem. Soc.*, 1999, **121**, 5302. (b) S. Accorsi, A. L. Barra, A. Caneschi, G. Chastanet, A. Cornia, A. C. Fabretti, D. Gatteschi, C. Mortalo, E. Olivieri, F. Parenti, P. Rosa, R. Sessoli, L. Sorace, W. Wernsdorfer and L. Zobbi, *J. Am. Chem. Soc.*, 2006, **128**, 4742.
6. C. Schlegel, E. Burzurí, F. Luis, F. Moro, M. Manoli, E.K. Brechin, M. Murrie and J. van Slageren, *Chem.–Eur. J.*, 2010, **16**, 10178.
7. L. Gregoli, C. Danieli, A. L. Barra, P. Neugebauer, G. Pellegrino, G. Poneti, R. Sessoli and A. Cornia, *Chem.–Eur J*, 2009, **15**, 6456.
8. A. Cornia, A. C. Fabretti, P. Garrisi, C. Mortalo, D. Bonacchi, D. Gatteschi, R. Sessoli, L. Sorace, W. Wernsdorfer and A. L. Barra, *Angew. Chem., Int. Ed.*, 2004, **43**, 1136.
9. (a) Y.-Y. Zhu, X. Guo, C. Cui, B.-W. Wang, Z. M. Wang and S. Gao, *Chem. Commun.*, 2011, **47**, 8049. (b) Y.-Y. Zhu, C. Cui, K. Qian, J. Yin, B.-W. Wang, Z.-M. Wang and S. Gao, *DaltonTrans*., 2014, **43**, 11897.
10. A. L. Spek, PLATON, A Multipurpose Crystallographic Tool, Utrecht University, The Netherlands, 2002.
11. J. M. Clemente-Juan, J. J. Borras-Almenar, E. Coronado, A. V. Palii and B. S. Tsukerblat, *Inorg. Chem.*, 2009, **48**, 4557.
12. M. P. Shores, J. J. Sokol and J. R. Long, *J. Am. Chem. Soc.*, 2002, **124**, 2279.
13. A. Cornia, R. Sessoli, L. Sorace, D. Gatteschi, A. L. Barra and C. Daiguebonne, *Phys. Rev. Lett.*, 2002, **89**, 257201.
14. W. Wernsdorfer, M. Murugesu and G. Christou, *Phys. Rev. Lett.*, 2006, **96**, 057208.
15. (a) A. L. Barra, A. Caneschi, A. Conia, D. Gatteschi, L. Gorini, L. P. Heiniger, R. Sessoli and L. Sorace, *J. Am. Chem. Soc.*, 2007, **129**, 10754. (b) L. Sorace, M. E. Boulon, P. Totaro, A. Cornia, J. Fernandes-Soares and R. Sessoli, *Phys. Rev. B*, 2013, **88**, 104407.
16. S. Stoll and A. Schweinger, *J. Magn. Reson.* 2006, **178**, 42.

[a] *Key Laboratory of Advanced Functional Materials and Devices, Anhui Province, School of Chemical Engineering, Hefei University of Technology, Hefei, Anhui, 230009, P. R. China.*
[b] *Beijing National Laboratory of Molecular Science, College of Chemistry and Molecular Engineering, State Key Laboratory of Rare Earth Materials Chemistry and Applications, Peking University, Beijing, 100871, P. R. China. E-mail: gaosong@pku.edu.cn*
[c] *1. Physikalisches Institut, Universität Stuttgart, Pfaffenwaldring 57, 70569 Stuttgart, Germany*
[d] *LNCMI-CNRS, 25 rue des Martyrs BP 166, 38042 Grenoble Cedex 9 France. E-mail: jiang@lncmi.cnrs.fr*
[e] *InstitutNéel, CNRS& UJF BP 166, 38042, Grenoble Cedex 9, France*
[f] *Institut für Physikalische Chemie, Universität Stuttgart, Pfaffenwaldring 55, 70569 Stuttgart, Germany, E-mail: slageren@ipc.uni-stuttgart.de*

† Electronic Supplementary Information (ESI) available: [details of any supplementary information available should be included here]. See DOI: 10.1039/b000000x/